Chloride ion penetration resistance of concrete containing fly ash and silica fume against combined freezing-thawing and chloride attack

Dezhi Wang[a,b,c,d*], Xiangming Zhou[a], Bo Fu[e] and Lirong Zhang[f]

[a]Department of Civil & Environmental Engineering, Brunel University London, Uxbridge, Middlesex UB8 3PH, United Kingdom

[b]College of Civil & Water Conservancy Engineering, Ningxia University, Yinchuan 750021, China

[c]Ningxia Water-efficient Irrigation Engineering Research Center, Yinchuan 750021, Ningxia, China

[d]Water Resources Engineering Research Center in Modern Agriculture in Arid Regions, Yinchuan 750021, China

[e]School of Civil Engineering, North Minzu University, Yinchuan 750021,China

[f]Henan Communication Vocational and Technical College, Zhengzhou 450015, China

Abstract:

Chloride ion penetration resistance (CPR) of concrete containing fly ash (FA)/silica fume (SF) against combined freezing-thawing and chloride attack was studied. The total charge passed, immersed in tap water and sodium chloride solution, subjected to 50 freezing-thawing cycles was evaluated. It was found that immersed in tap water, SF had more evident improvement on concrete's resistance to combined effects than

*Corresponding author at: Department of Civil & Environmental Engineering, Brunel University London, Uxbridge, Middlesex UB8 3PH, United Kingdom. E-mail address: dezhi.wang@brunel.ac.uk (Dezhi Wang).

FA. Sodium chloride solution immersion for 41d prior to test was more aggressive than tap water. After 50 freezing-thawing cycles, CPR of concrete with FA increased, while that with SF decreased. Interaction between freezing-thawing and chloride attack accelerated concrete deterioration.

Keywords: concrete durability; chloride penetration resistance; total charge passed; fly ash; silica fume; freezing-thawing; chloride attack; sodium chloride concentration; interaction between freezing-thawing and chloride attack

1. Introduction

Concrete is versatile and the most widely used construction material in the world. But owning to aggressive marine exposure environment and the extensive use of de-icing salts in many countries, chloride induced corrosion becomes one of the most common causes of degradation of reinforced concrete structures [1-4]. The first effect of chloride ions is physical salt attack leading to surface cracking and scaling which is similar in appearance to freezing-and-thawing damage and total disintegration of low-quality concrete [5]. Another effect is that chloride ions are the most important cause of corrosion of embedded rebar. When chloride ions penetrate concrete cover and arrive at reinforcement bars, as their amount accumulates, the passive film may break down (i.e. de-passivation) and corrosion of embedded rebar can then initiate [6, 7]. The accumulation of corrosion products can build up the swelling pressure around the rebar resulting in cracking or spalling of concrete[8], which in turn facilitates the

ingress of moisture, oxygen, and chlorides to the rebar and accelerates rebar corrosion [9]. Pitting corrosion is another threat to RC structures in a chloride environment [10] and is a type of more serious corrosion on structural safety than general corrosion[11, 12], since it has resulted in quite high loss of cross-sectional area of reinforcement bars [13] and structural damages[14], or in extreme situations, the final collapse of the structure.

Chloride penetration in concrete can be characterized by the chloride diffusion coefficient and the binding ability of matrix-forming solids [15]. In concrete, chlorides can be chemically bound with cement's C3A or C4AF phases (e.g., Friedel's salt) [16], or physically hold to the surface of hydration products (e.g., adsorption on C-S-H) [3, 17]. Chloride diffusion depends on pure diffusion for water-saturated concrete and capillary absorption of salty water for non-saturated concrete [18].

Recently, there are several studies reported in literature on the transport of chloride ions in concrete and numerical models developed to simulate the process [7, 19-22]. Meanwhile, chloride penetration into concrete is governed by many factors. Due to the chemical and physical bond between chloride ion and hydrated product of cement changing the micro-structure, the chloride diffusion coefficient changes during the exposure period and decreases with an increased period of exposure [23-26]. Nobuaki [27] and Page [28] both studied chloride ions diffusion in concrete at different temperatures and the results reveal that the rates of diffusion of Cl^- in concrete rises with increases in temperature. In real environments, concrete structures are subjected to various environmental factors acting in a combined and possibly synergistically

66 physical and chemical manner to accelerate the destruction process. Therefore, it is
67 significant to study chloride resistance of concrete under combined deteriorating
68 factors to obtain sufficient information on concrete durability. Chloride penetration
69 and carbonation of concrete are often considered to be the most significant coupled
70 deterioration factors and numerous studies have taken both factors into account in
71 assessing concrete durability [29-35]. As reported by Chindaprasirt [29] , Tumidajski
72 [31] and Houst [36], carbonation decreases chloride penetration and diffusivity in
73 ordinary Portland cement (OPC) mortar and concrete. While other test results [30, 34,
74 35] indicate that chloride penetration is accelerated when the carbonation process is
75 combined with the chloride ingress due to liberate bound chloride. The carbonation
76 effect on chloride penetration is controversial and considered to depend on the types
77 and mix proportions of concretes [29, 33, 35]. Initial cracks in concrete significantly
78 influence chloride penetration and the influence of crack width and depth has been
79 experimentally and numerically studied. It is clear that chloride transport is very rapid
80 along and across crack boundaries [37]. Concrete specimens are made with artificial
81 cracks by means of the positioning and removal after approximately 4 h of thin copper
82 sheets inside the specimen[38]. These copper sheets have a thickness of 0.2 mm, 0.3
83 mm or 0.5 mm. The copper sheets are placed at a depth in the concrete specimen of 5
84 mm, 10 mm, 15 mm or 20 mm. The test results also indicate that the penetration depth
85 increases with an increasing notch depth and that the influence of notch depth is more
86 pronounced for longer test duration while the influence of notch width is not clear [38,
87 39]. The chloride permeability of a concrete is influenced significantly by loading

style and critical stress [40-43]. The application of static loading up to 90% of the ultimate strength had little effect on chloride permeability while load repetitions at the maximum stress levels of 60% or more caused chloride permeability to increase significantly [41].

In addition, drying and wetting cycles are always identified as the most unfavorable environment condition for reinforced concrete structure subjected to chloride-induced deterioration processes and it accelerates the ingress of chloride ions and affects concrete durability [44, 45].

Investigations on chloride penetration resistance of concrete have also been conducted in concrete science and engineering community, but studies on the effects of chloride ion on deterioration of concrete with FA and SF under combined freezing-thawing and chloride attack is very limited in literature. Rapid chloride permeability test (RCPT) is the most widely specified durability test method and is standardized by ASTM. The total charge passed (in Coulombs), the result of RCPT, provides a rapid indication of its resistance to the penetration of chloride ions and is calculated via Equation (1). In this research, concrete's total charge passed, immersed in tap water and sodium chloride solutions, subjected to 50 freezing-thawing cycles was evaluated. The influence of FA and SF replacement level of OPC and sodium chloride concentration on durability of concrete under the combined freezing-thawing and chloride attack was also investigated.

2. Experimental program

2.1 Materials

42.5 R Portland cement, manufactured by Saima Cement Manufacturing Company of Ningxia, China conforming to EN197-1:2009, was used for preparing concrete in this research and its physical and mechanical properties are listed in Table 1. Table 2 presents the chemical composition of the cement, FA and SF used in this study as partial replacement of OPC. Crushed limestone aggregates were used as coarse aggregates and washed mountain sand as fine aggregates, and the sieving curves are presented in Fig.1. The fineness modulus of fine aggregates was evaluated conforming to ASTM C136-01 and the results are presented in Table 3. Tap water was used for mixing concrete. A commercially available naphthalene-based water reducer (i.e. FDN, produced by MUHU Concrete Admixture Ltd.) was used to keep concrete slump between 80 and 100 mm and its chemical characteristics are listed in Table 4. Sodium chloride anhydrous with 99.5% purity and sodium hydroxide anhydrous with 99.0% purity were used for making chlorate solutions as the chloride attack source.

Table 1

Physical and mechanical properties of OPC used for this research

	80μm sieving residue (%)	Water requirement of normal consistency (%)	Initial setting time (min)	Final setting time (min)	Compressive strength (MPa)		Flexural strength (MPa)		soundness
					3 days	28 days	3 days	28 days	
Experimental result	1.60	27.3	90	135	26.0	45.9	6.0	8.3	qualified

Table 2

Chemical compositions of Portland cement, fly ash (FA) and silica fume (SF)

Chemical composition	SiO_2	Al_2O_3	Fe_2O_3	CaO	MgO	SO_3	Na_2O+K_2O
Cement weight percent (%)	22.04	5.77	3.36	66.43	0.45	0.00	0.51
FA weight percent (%)	31.93	8.98	5.2	43.87	2.14	0.2	1.95
SF weight percent (%)	97.2	0.26	0.45	0.17	--	--	--

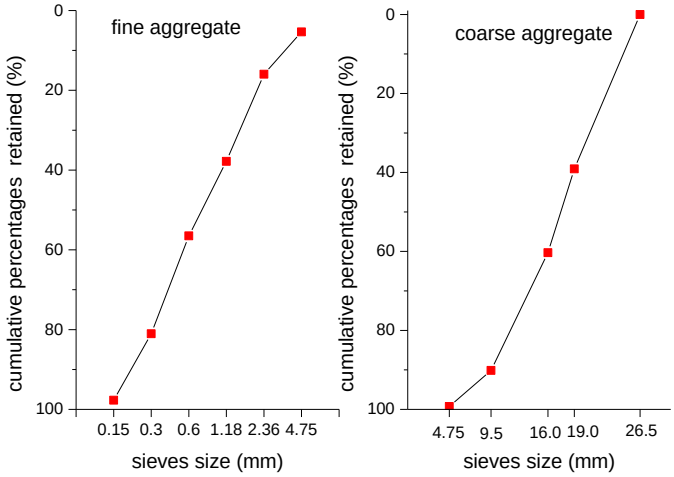

Fig. 1 Sieving curves of fine and coarse aggregates

Table 3

Physical characteristics of aggregates

	Apparent density (kg/m^3)	Bulk density (kg/m^3)	Crushing value index (%)	Maximum size(mm)	Fineness modulus	Dust content (%)
Fine aggregates	2735	1566	--	5	2.78	0.85
Coarse aggregates	2684	1470	7.8	20	--	0.12

Table 4

Chemical characteristics of naphthalene-based water reducer

PH	Chloride ion content (%)	Na_2SO_4 content (%)
8.1	0.1	2.5

2.2 Mix proportion and specimen preparation

The actual mix proportions in terms of 1 m^3 concrete for the mixtures investigated in this study are given in Table 5. In order to investigate the effect of FA and SF on the resistance of concrete to combined freezing-thawing and chloride attack, the total binder content of all mixtures was 500 kg/m³ according to Wu[46] and concrete mixtures were prepared with w/b ratios of 0.38 and 0.33, respectively. In each group, concrete mixtures with three different FA contents (i.e. of 10%, 15% and 25% by weight of cementitious materials (i.e. OPC + FA + SF)), three different silica fume contents (i.e. of 5%, 8% and 11% also by weight of cementitious materials) as partial replacement of OPC were prepared and tested.

Cubic specimens with the dimensions of 100 ×100 ×100 mm^3 were prepared for measuring compressive strength and cylinder specimens with (100±1) mm in diameter and (50±2) mm in height for assessing Chloride Ion penetration resistance. Concrete mixtures were prepared by a single horizontal-axis forced mixer. After moulded, concrete specimens were placed in a curing room with temperature of (20±5)°C for 24 hour. Then they were demoulded and immersed in tap water with temperature of (20±2)°C for another 27 days, which is referred as 28 days standard curing in this paper. Concrete specimens for measuring compressive strength and Chloride Ion penetration resistance were prepared for assessing long-term performance and durability of ordinary concrete.

Table 5

Mix proportions in kg/m^3 (except w/b) of concretes investigated in this study

	w/b	Fly ash	Silica fume	OPC	Coarse aggregates	Fine aggregates	Water
C-8	0.38	0	0	500	1094	616	190
FA10-8	0.38	50	0	450	1094	616	190
FA15-8	0.38	75	0	425	1094	616	190
FA25-8	0.38	125	0	375	1094	616	190
SF5-8	0.38	0	25	475	1094	616	190
SF8-8	0.38	0	40	460	1094	616	190
SF11-8	0.38	0	55	445	1094	616	190
C-3	0.33	0	0	500	1145	590	165
FA10-3	0.33	50	0	450	1145	590	165
FA15-3	0.33	75	0	425	1145	590	165
FA25-3	0.33	125	0	375	1145	590	165
SF5-3	0.33	0	25	475	1145	590	165
SF8-3	0.33	0	40	460	1145	590	165
SF11-3	0.33	0	55	445	1145	590	165

2.3 Chloride ion penetration resistance assessment

For assessing effects of chloride concentration on Chloride Ion penetration resistance of concrete, cylindrical concrete specimens with (100±1) mm in diameter and (50±2) mm in height cured standardly for 28 days were then immersed in tap water and designated solution (i.e. 4% and 10% by wt. sodium chloride solutions), respectively, for another 41 days. Conforming to ASTM C1202-12, the rapid chloride penetration test (RCPT) was proceeded as following. First, cylindrical concrete specimens were placed in a vacuum pump with its pressure decreased to less than 5000 Pa within 5 minutes and maintained the pressure for 3 hours; then concrete specimens were immersed in distilled water at the vacuum pressure for 1 hour followed by being immersed for (18±2) hours at normal ambient pressure; and finally one side of the cylindrical specimen containing the top surface was filled with 3.0 % NaCl solution

and the other side of with 0.3 mol/L NaOH solution. During the 6 hours RCPT test, temperatures of the specimen and the solutions were targeted to be between 20 and 25°C and they were recorded once every 5 minutes to ensure the target was reached. The total charge passed during the RCPT test was measured and calculated via Equation (1).

$$Q = 900\left(I_0 + 2I_{30} + 2I_{60} + \cdots + 2I_t + \cdots + 2I_{300} + 2I_{330} + I_{360}\right) \quad (1)$$

where Q in Coulombs is the total charge passed; I_0 in Amperes current immediately after voltage is applied; I_t in Amperes current at t min after voltage is applied.

2.4 Freezing-thawing resistance assessment

To assess concrete's resistance to combined freezing-thawing and chloride attack, cylindrical concrete specimens with (100±1) mm in diameter and (50±2) mm in height were cured standardly for 56 days, then they were subjected to rapid freezing-thawing cycle test in tap water and designated solution (i.e. 4% and 10% by wt. sodium chloride solutions), respectively. Conforming to ASTM C666/C666M–03, a standard rapid freezing-thawing cycle lasted for 6 hours and was proceeded as following: a cylindrical concrete specimen was frozen in the tap water or designated sodium sulfate solution for 3 hours at -18(±2)°C, and subsequently it was thawed for 3 hours in water at 5(±2)°C. All concrete specimens were subjected to 50 such freezing-thawing cycles. After that the RCPT was conducted. The deterioration coefficient of total charge passed during the RCPT test was calculated via Equation (2).

$$\lambda = \frac{Q_c}{Q_s} \quad (2)$$

where λ in % the deterioration coefficient of total charge passed; Q_c and Q_s in Coulombs the total charge passed of a concrete specimen after subjected to combined freezing-thawing and chloride attack and to solely freezing-thawing attack in tap water, respectively.

2.5 Observation under the Scanning Electron Microscopy (SEM)

The morphology and microstructure observation under SEM (KYKY2800B) from Ningxia University were carried out on the specimens in order to understand the influence of freezing-thawing and chloride attack. SEM specimens were dried in drying oven for 48 hours at (80±5) °C, and subsequently specimens' surfaces were coated using a gold sputter coater to eliminate effects of charging during micrograph collection.

3. Results and discussion

3.1 FA or SF dosage and chloride ion penetration resistance

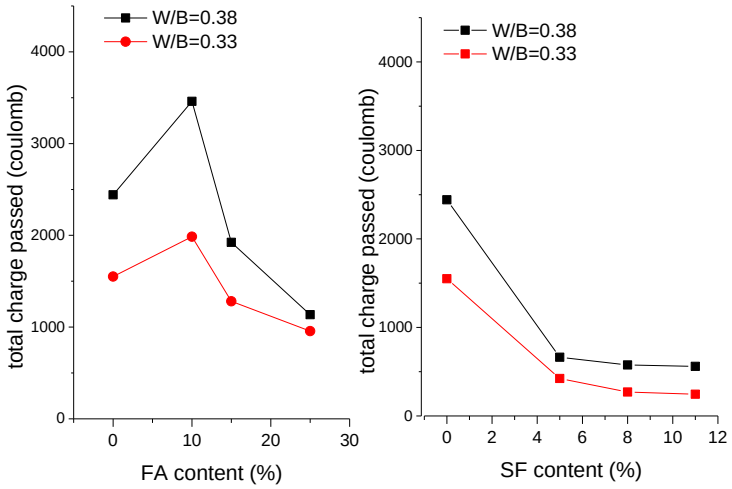

Fig.2 Total charge passed of concretes with various FA and SF contents

Measured total charge passed of the concrete specimens with various FA and SF contents after immersed in tap water for 69 days (i.e. 28 days + 41 days) is presented in Fig.2. The test results demonstrated that in general concrete's total charge passed actually decreased, as the FA or SF dosage increased and it was obvious that SF had more evident improvement on concrete chloride penetration resistance (i.e. on reducing total charge passed) than FA. Cured in tap water, concrete specimens with 10% FA had the highest total charge passed (i.e. 3460.1C in case of the water-to-binder ratio of 0.38 and 1985.2 C in case of the water-to-binder of 0.33) than concrete specimens with other FA dosages, while concrete with 25% FA had the lowest value (i.e. 1135.1C with a water-to-binder ratio of 0.38 and 955.8C with a water-to-binder ratio of 0.33). In case of concretes with SF, the total charges passed were all less than 1000C and the higher chloride penetration resistance can be found from concretes with higher FA and SF dosage which exhibited lower total charge

passed. According to ASTM C1202, C-8 and C-3 mixtures were classified as moderate (2000-4000 coulombs) and low (1000-2000 coulombs), respectively, level of chloride ion penetrability, FA25-8 as low (1000-2000 coulombs) level of chloride ion penetrability, while FA25-3 and all concretes with SF as very low (100-1000 coulombs) level of chloride ion penetrability.

3.2 Sodium chloride attack and chloride ion penetration resistance

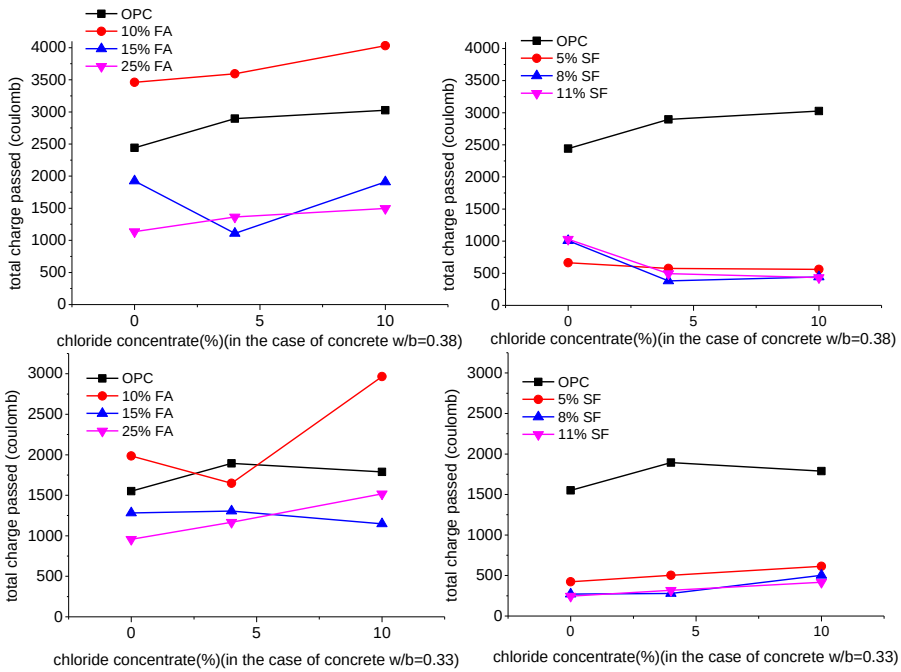

Fig.3 Total charge passed of concretes immersed in sodium chloride solutions with various concentrations

The cylindrical concrete specimens were cured standardly for 28 days, then they were immersed in 0, 4% and 10%, respectively, sodium chloride solutions by wt. % for another 41 days and chloride ion penetration test was conducted immediately after 41

246 days immersion. Fig.3 presents the evolution of the total charge passed of concretes
247 exposed to sodium chloride solutions with various concentrations. Similar trend was
248 observed in concretes with different FA or SF contents. The results indicated that
249 under the two water-to-binder ratios (i.e. w/b = 0.38 and 0.33), sodium chloride
250 solution immersion for 41 days prior to the test was more aggressive than tap water
251 and 10% sodium chloride solution caused the largest rise in total charge passed. In the
252 case of w/b of 0.38, total charge passed of concretes with 0, 10%, 15% and 25% by
253 weight FA immersed in 10% sodium chloride solution had raised to 124.0%, 116.5%,
254 99.2% and 131.9 %, respectively, of their corresponding original value, and in the
255 case of w/b =0.33, the counterpart value was 115.4%, 149.4%, 89.6% and 158.8%,
256 respectively. As for w/b =0.38 concretes with 5%, 8% and 11% SF by weight, total
257 charge passed had raised to 155.2%, 85.8% and 77.4 %, respectively, of their
258 corresponding original value; and for w/b =0.33 concretes, the counterpart value was
259 144.8%, 185.9% and 170.3%, respectively.
260 In addition, 10% FA decreased chloride penetration resistance and had higher total
261 charge passed than OPC concrete not only in tap water but also in sodium chloride
262 solution while 15-25% FA can significantly improve chloride penetration resistance in
263 the same condition. All of the three SF dosages played more actively important role
264 than FA in raising the chloride penetration resistance and all concrete mixtures with
265 SF were at very low (100-1000 coulombs) level of total charge passed, indicating very
266 low level of chloride ion penetrability.
267

3.3 50 freezing-thawing cycles and chloride ion penetration resistance

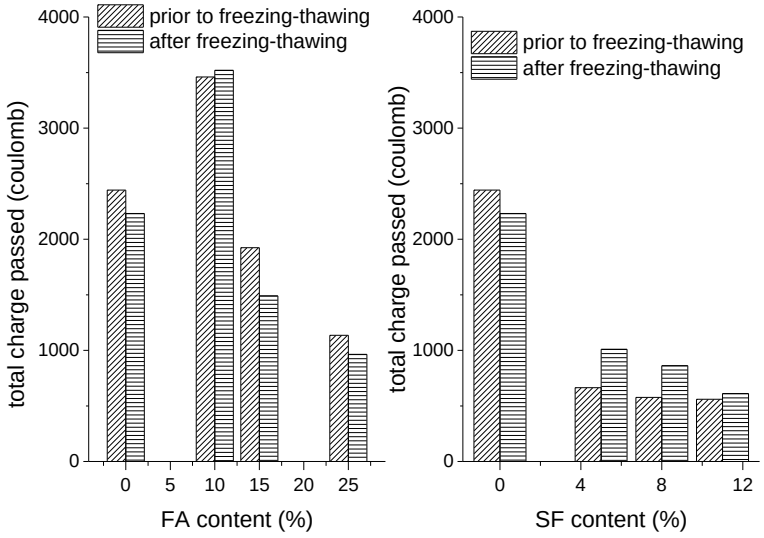

Fig.4 Total charge passed of concretes after 50 freezing-thawing cycles.

The cylindrical concrete specimens were cured under standard curing condition for 56 days and then subjected to freezing-thawing cycles in tap water, 4% and 10% sodium chloride solutions up to 50 cycles, which lasted around 13 days, and subsequently chloride ion penetration test were conducted. The total charge passed of various concretes exposed to tap water under freezing-thawing cycles are depicted in Fig.4 (for concretes with w/b=0.38). There was a significant decrease in total charge passed ranged from 8.6% to 22.6% over the test period for the concrete with 15% and 25% FA by weight, respectively, while a slight increase by 1.7% for concrete with 10% FA by weight. In the case of concrete with SF, the total charge passed increased by 52.2%, 49.7% and 9.0% at the SF content of 5%, 8% and 11% by weight, respectively. It can be concluded that under 50 freezing-thawing cycles, chloride ion penetration

resistance of concrete with FA increased while that of concrete with SF decreased.

3.4 Chloride ion penetration resistance against combined freezing-thawing and chloride attack

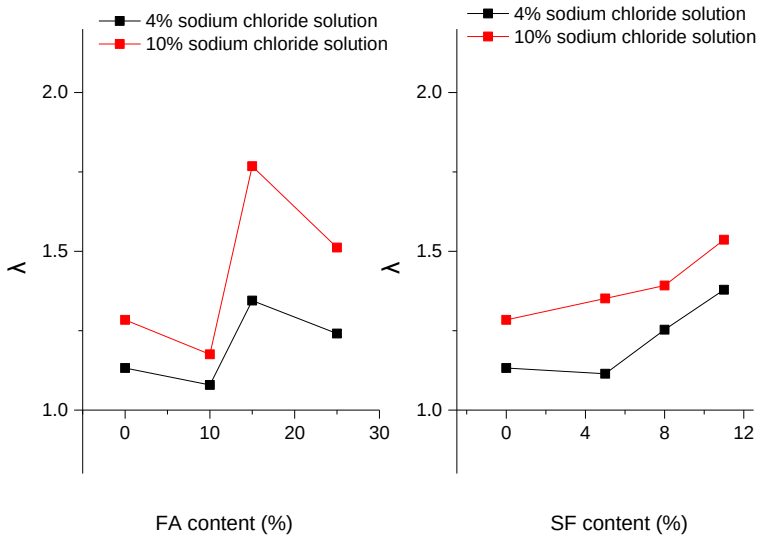

Fig.5 Deterioration coefficient of total charge passed of concretes exposed to tap water and sodium chloride solution after 50 freezing-thawing cycles.

Concrete deterioration was associated with the interaction between freezing-thawing and chloride attack. Via Equation (2), if $\lambda>1$, it means the interaction accelerates concrete deterioration. If $\lambda<1$, the interaction retards concrete deterioration. When λ becomes larger or smaller, the accelerating or retarding effect on concrete deterioration becomes more significant. In Fig.5 the interaction between freezing-thawing and chloride attack accelerated the deterioration of all concrete specimens, 10% sodium chloride solution demonstrated higher deterioration effect than 4% solution. In the case of concretes with 15-25% FA, their λ values were

obviously higher than those of OPC concretes, while in the case of concretes with SF, λ increased as the SF dosage increased. It can be concluded that when the FA dosage was more than 15% or SF dosage more than 8%, both by weight, the acceleration effect of the interaction between freezing-thawing and chloride attack on concrete deterioration was more significant, and these concretes were more vulnerable to the interaction and had the lower chloride ion penetration resistance against combined freezing-thawing and chloride attack.

3.5. SEM

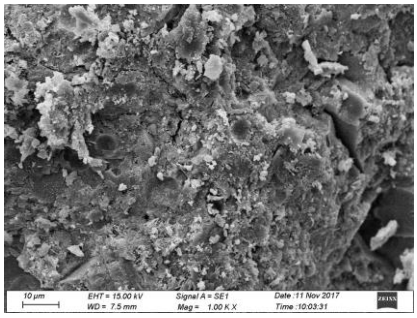

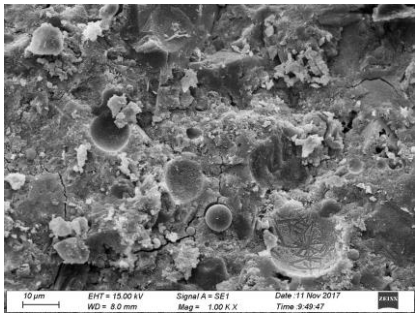

(a) FA25-3 (b) FA25-3

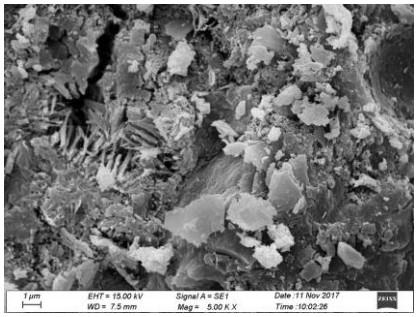

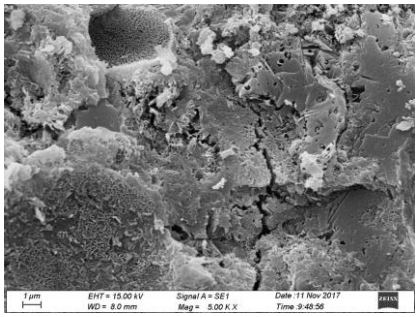

(c) FA25-3 (d) FA25-3

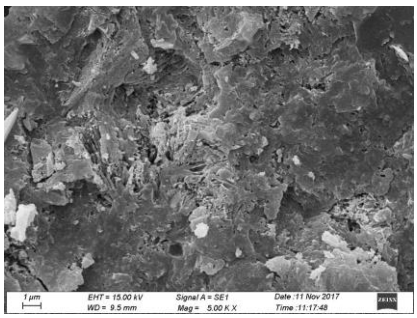

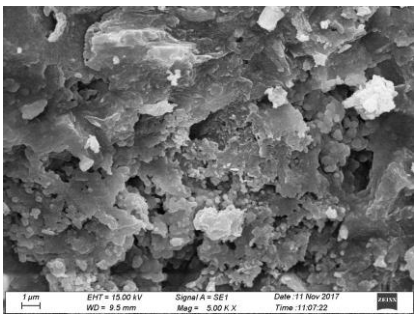

(e) SF8-3 (f) SF8-3

Figs.6 SEM images of concrete with 25% FA, 8% SF by weight exposed to tap water ((a), (c) and (e) and 10% sodium chloride solution ((b), (d) and (f))

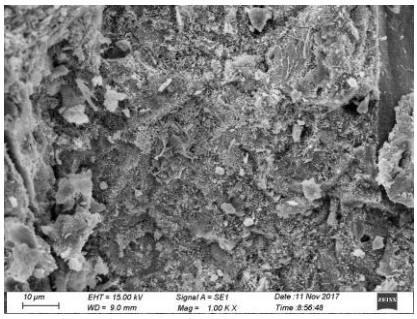

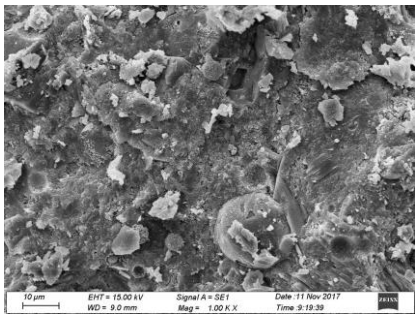

(a) FA25-8 (b) FA25-8

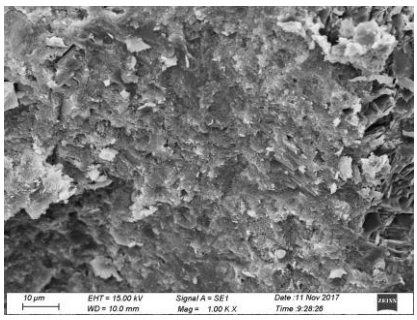

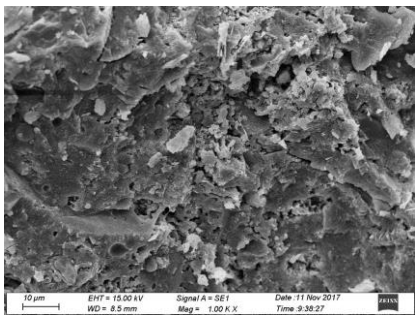

(c) SF8-8 (d) SF8-8

Figs.7 SEM images of concrete with 25% FA, 8% SF by weight exposed to tap water ((a) and (c)) and to 10% sodium chloride solution ((b) and (d)) after 50 freezing-thawing cycles

Figs.6 and Figs.7 present SEM images of concrete specimens at a depth of 5mm. When concretes were exposed to tap water, there were no clear microcracks resulting in a very compact microstructure, and this was the result of the pozzolanic reaction (i.e. Figs. 6(a) and (e). The use of pozzolanic materials (i.e. FA and SF) increases the

CSH, reduce the CH and the porosity in the cementitious matrix [47, 48]. The decrease of total charge passed of concrete with pozzolanic materials was attributed to the decrease of the porous system which is directly related to the electrical resistivity [49] and the low water to binder ratio.

When concretes were exposed to sodium chloride solution up to 41 days, it can be observed that there were not obvious differences in microstructures up to 1000 times magnification (i.e. Figs.6 (a) and (b)), while at 5000 times magnification the concrete specimen with 25% FA and 8% SF exposed to tap water had smaller pore and denser structure than those to 10% sodium chloride solution (i.e. Figs.6 (c), (d), (e) and (f)).

When concrete specimens were exposed to 10% sodium chloride solution solutions up to 50 freezing-thawing cycles (i.e. Figs.7), there were two different trends. Concrete specimens with 25% by weight FA replacing OPC possessed compacter microstructure than those in tap water, while the microstructure of the one with 8% by weight SF replacing OPC would be looser after 50 freezing-thawing cycles.

4. Conclusions

Chloride ion penetration of concretes with w/b of 0.38 and 0.33 containing FA or SF against combined freezing-thawing and chloride attack was investigated in this study. The following conclusions can be drawn based on the experimental results.

(1) Immersed in tap water, concrete's total charge passed actually decreased as the FA or SF dosage increased and, in comparison, SF had more evident improvement on concrete chloride penetration resistance than FA. It was

clearly indicated that 15% and 25% by weight FA and all SF dosages were more effective to reduce concrete total charge passed and to enhance chloride penetration resistance. All concretes with SF were classified as at very low (100-1000 coulombs) level of chloride ion penetrability.

(2) Sodium chloride solution immersion was more aggressive to concrete than tap water and 10% sodium chloride solution caused the lowest chloride penetration resistance. In addition, 15-25% by weight FA can significantly improve chloride penetration resistance not only in tap water but also in sodium chloride solution. All of the three SF dosages played more actively important role than FA in raising the chloride penetration resistance and all concretes with SF were at very low (100-1000 coulombs) level of chloride ion penetrability when immersed in sodium chloride solution.

(3) After 50 freezing-thawing cycles in tap water, chloride ion penetration resistance of concrete with FA increased, while that of concrete with SF decreased.

(4) The interaction between freezing-thawing and chloride attack accelerated the deterioration of all concrete specimens and 10% sodium chloride solution demonstrated higher deterioration effect than 4% solution. Concretes with more than 15% FA or 8% SF by weight replacing OPC had lower chloride ion penetration resistance against combined freezing-thawing and chloride attack

Acknowledgement

The authors would like to acknowledge the National Natural Science Foundation of China (through the grant 51368049 and 51668001), Ningxia First Class Discipline Project (through the grant NXYLXK2017A03) and Ningxia University Subject Development Project for sponsoring this research. The first author would also like to acknowledge the China Scholarship Council for sponsoring his one-year visit to Brunel University London where this paper was completed.

References

[1] U. Angst, B. Elsener, C.K. Larsen, O. Vennesland, Critical chloride content in reinforced concrete - A review, Cem. Concr. Res. 39(12) (2009) 1122-1138.

[2] L. Basheer, J. Kropp, D.J. Cleland, Assessment of the durability of concrete from its permeation properties: A review, Constr. Build. Mater. 15(2-3) (2001) 93-103.

[3] X. Shi, N. Xie, K. Fortune, J. Gong, Durability of steel reinforced concrete in chloride environments: An overview, Constr. Build. Mater. 30 (2012) 125-138.

[4] M.G. Stewart, D.V. Rosowsky, Time-dependent reliability of deteriorating reinforced concrete bridge decks, Struct. Saf. 20(1) (1998) 91-109.

[5] A.C. 201, Guide to durable concrete (ACI 201.2R-08), American concrete institute, MI, 2008.

[6] D.W.S. Ho, R.K. Lewis, Carbonation of concrete and its prediction, Cem. Concr. Res. 17(3) (1987) 489-504.

[7] Z.P. Bazant, Physical model for steel corrosion in concrete sea structures-theory, ASCE J Struct Div 105(6) (1979) 1137-1153.

395 [8] C. Cao, M.M.S. Cheung, Non-uniform rust expansion for chloride-induced pitting
396 corrosion in RC structures, Constr. Build. Mater. 51 (2014) 75-81.
397 [9] L. Bertolini, B. Elsener, P. Pedeferri, E. Redaelli, R.B. Polder, Corrosion of steel in
398 concrete: prevention, diagnosis, repair, John Wiley & Sons.2013.
399 [10] M.S. Darmawan, Pitting corrosion model for reinforced concrete structures in a
400 chloride environment, Mag. Concr. Res. 62(2) (2010) 91-101.
401 [11] G.C. Marano, G. Quaranta, M. Mezzina, Fuzzy Time-Dependent Reliability
402 Analysis of RC Beams Subject to Pitting Corrosion, J. Mater. Civ. Eng. 20(9) (2008)
403 578-587.
404 [12] J. Wu, W. Wu, Study on wireless sensing for monitoring the corrosion of
405 reinforcement in concrete structures, Measurement 43(3) (2010) 375-380.
406 [13] M.G. Stewart, Spatial variability of pitting corrosion and its influence on
407 structural fragility and reliability of RC beams in flexure, Struct. Saf. 26(4) (2004)
408 453-470.
409 [14] E. Mazario, R. Venegas, P. Herrasti, M.C. Alonso, F.J. Recio, Pitting corrosion and
410 stress corrosion cracking study in high strength steels in alkaline media, Journal of
411 Solid State Electrochemistry 20(4) (2016) 1223-1227.
412 [15] C. Andrade, R. Buják, Effects of some mineral additions to Portland cement on
413 reinforcement corrosion, Cem. Concr. Res. 53 (2013) 59-67.
414 [16] U.A. Birnin-Yauri, F.P. Glasser, Friedel's salt, Ca2Al(OH)6(Cl,OH)·2H2O: Its solid
415 solutions and their role in chloride binding, Cem. Concr. Res. 28(12) (1998)
416 1713-1723.

417 [17] A. Delagrave, J. Marchand, J.-P. Ollivier, S. Julien, K. Hazrati, Chloride binding
418 capacity of various hydrated cement paste systems, Adv. Cem. Based Mater. 6(1)
419 (1997) 28-35.
420 [18] E.P. Nielsen, M.R. Geiker, Chloride diffusion in partially saturated cementitious
421 material, Cem. Concr. Res. 33(1) (2003) 133-138.
422 [19] M.D.A. Thomas, P.B. Bamforth, Modelling chloride diffusion in concrete: Effect of
423 fly ash and slag, Cem. Concr. Res. 29(4) (1999) 487-495.
424 [20] G.K. Glass, N.R. Buenfeld, The influence of chloride binding on the chloride
425 induced corrosion risk in reinforced concrete, Corrosion Sci. 42(2) (2000) 329-344.
426 [21] C.A. Apostolopoulos, V.G. Papadakis, Consequences of steel corrosion on the
427 ductility properties of reinforcement bar, Constr. Build. Mater. 22(12) (2008)
428 2316-2324.
429 [22] C. Cao, 3D simulation of localized steel corrosion in chloride contaminated
430 reinforced concrete, Constr. Build. Mater. 72 (2014) 434-443.
431 [23] P.S. Mangat, M.C. Limbachiya, Effect of initial curing on chloride diffusion in
432 concrete repair materials, Cem. Concr. Res. 29(9) (1999) 1475-1485.
433 [24] M.D.A. Thomas, J.D. Matthews, Performance of pfa concrete in a marine
434 environment - 10-year results, Cem Concr Compos 26(1) (2004) 5-20.
435 [25] S.-W. Pack, M.-S. Jung, H.-W. Song, S.-H. Kim, K.Y. Ann, Prediction of time
436 dependent chloride transport in concrete structures exposed to a marine
437 environment, Cem. Concr. Res. 40(2) (2010) 302-312.
438 [26] K. Audenaert, Q. Yuan, G. De Schutter, On the time dependency of the chloride

439 migration coefficient in concrete, Constr. Build. Mater. 24(3) (2010) 396-402.
440 [27] N. Otsuki, M.S. Madlangbayan, T. Nishida, T. Saito, M.A. Baccay, Temperature
441 Dependency of Chloride Induced Corrosion in Concrete, Journal of Advanced
442 Concrete Technology 7(1) (2009) 41-50.
443 [28] C.L. Page, N.R. Short, A. El Tarras, Diffusion of chloride ions in hardened cement
444 pastes, Cem. Concr. Res. 11(3) (1981) 395-406.
445 [29] P. Chindaprasirt, S. Rukzon, V. Sirivivatnanon, Effect of carbon dioxide on chloride
446 penetration and chloride ion diffusion coefficient of blended Portland cement mortar,
447 Constr. Build. Mater. 22(8) (2008) 1701-1707.
448 [30] X.-m. Wan, F.H. Wittmann, T.-j. Zhao, H. Fan, Chloride content and pH value in
449 the pore solution of concrete under carbonation, Journal of Zhejiang University
450 SCIENCE A 14(1) (2013) 71-78.
451 [31] P.J. Tumidajski, G.W. Chan, Effect of sulfate and carbon dioxide on chloride
452 diffusivity, Cem. Concr. Res. 26(4) (1996) 551-556.
453 [32] I.S. Yoon, Simple approach to calculate chloride diffusivity of concrete
454 considering carbonation, Comput. Concr. 6(1) (2009) 1-18.
455 [33] V.T. Ngala, C.L. Page, Effects of carbonation on pore structure and diffusional
456 properties of hydrated cement pastes, Cem. Concr. Res. 27(7) (1997) 995-1007.
457 [34] M.K. Lee, S.H. Jung, B.H. Oh, Effects of Carbonation on Chloride Penetration in
458 Concrete, ACI Mater. J. 110(5) (2013) 559-566.
459 [35] C.F. Yuan, D.T. Niu, D.M. Luo, Effect of carbonation on chloride diffusion in fly ash
460 concrete, Disaster Adv. 5(4) (2012) 433-436.

461 [36] Y.F. Houst, F.H. Wittmann, Depth profiles of carbonates fonned during natural
462 carbonation, Cem. Concr. Res. 32(12) (2002) 1923-1930.
463 [37] T. Ishida, P.O.N. Iqbal, H.T.L. Anh, Modeling of chloride diffusivity coupled with
464 non-linear binding capacity in sound and cracked concrete, Cem. Concr. Res. 39(10)
465 (2009) 913-923.
466 [38] L. Marsavina, K. Audenaert, G. Schutter, N. Faur, D. Marsavina, Experimental and
467 numerical determination of the chloride penetration in cracked concrete, Constr.
468 Build. Mater. 23(1) (2009) 264-274.
469 [39] B. Šavija, J. Pacheco, E. Schlangen, Lattice modeling of chloride diffusion in
470 sound and cracked concrete, Cem Concr Compos 42 (2013) 30-40.
471 [40] C.C. Lim, N. Gowripalan, V. Sirivivatnanon, Microcracking and chloride
472 permeability of concrete under uniaxial compression, Cem Concr Compos 22(5)
473 (2000) 353-360.
474 [41] M. Saito, H. Ishimori, Chloride Permeability of Concrete under Static and
475 Repeated Compressive Loading, Cem. Concr. Res. 25(4) (1995) 803-808.
476 [42] M.K. Rahman, W.A. Al-Kutti, M.A. Shazali, M.H. Baluch, Simulation of Chloride
477 Migration in Compression-Induced Damage in Concrete, J. Mater. Civ. Eng. 24(7)
478 (2012) 789-796.
479 [43] H.L. Ye, X.Y. Jin, C.Q. Fu, N.G. Jin, Y.B. Xu, T. Huang, Chloride penetration in
480 concrete exposed to cyclic drying-wetting and carbonation, Constr. Build. Mater. 112
481 (2016) 457-463.
482 [44] H. Ye, N. Jin, X. Jin, C. Fu, Model of chloride penetration into cracked concrete

483 subject to drying–wetting cycles, Constr. Build. Mater. 36 (2012) 259-269.
484 [45] S.J.H. Meijers, J. Bijen, R. de Borst, A.L.A. Fraaij, Computational results of a
485 model for chloride ingress in concrete including convection, drying-wetting cycles
486 and carbonation, Mater. Struct. 38(276) (2005) 145-154.
487 [46] Wu. Zhongwei, L. Huizhen, The high performance concrete, China Railway Press,
488 Beijing, China, 1999.
489 [47] V. Corinaldesi, G. Moriconi, Influence of mineral additions on the performance of
490 100% recycled aggregate concrete, Constr. Build. Mater. 23(8) (2009) 2869-2876.
491 [48] W. Sun, Y. Zhang, S. Liu, Y. Zhang, The influence of mineral admixtures on
492 resistance to corrosion of steel bars in green high-performance concrete, Cem. Concr.
493 Res. 34(10) (2004) 1781-1785.
494 [49] R. Corral-Higuera, S.P. Arredondo-Rea, M.A. Neri-Flores, J.M. Gomez-Soberon, J.L.
495 Almaral-Sanchez, J.H. Castorena-Gonzalez, A. Martinez-Villafane, F.
496 Almeraya-Calderon, Chloride Ion Penetrability and Corrosion Behavior of Steel in
497 Concrete with Sustainability Characteristics, Int. J. Electrochem. Sci. 6(4) (2011)
498 958-970.
499